

# CHARACTERISATION OF THIN CHITOSAN FILMS FOR GUIDED TISSUE REGENERATION PURPOSES

Katarzyna Lewandowska<sup>1\*</sup>, Gabriel Furtos<sup>2</sup>

<sup>1</sup>*Department of Chemistry of Biomaterials and Cosmetics, Faculty of Chemistry, Nicolaus Copernicus University in Toruń, 7 Gagarin Street, 87-100 Toruń Poland, e-mail: reol@umk.pl*

<sup>2</sup>*Department of Dental Materials, Raluca Ripan Institute of Research in Chemistry, Babes-Bolyai University, 30 Fantanele Street, 400294, Cluj-Napoca, Romania*

## **Abstract**

*The morphology and structure of thin films containing chitosan (Ch) with montmorillonite (MMT) were characterised by scanning electron microscopy (SEM), atomic force microscopy (AFM) and attenuated total reflectance Fourier transform infrared spectroscopy (ATR-FTIR). Thin films of two chitosan samples and a composition of chitosan with montmorillonite were formed by casting methods from acetic acid solutions and were soaked in a simulated body fluid (SBF) solution at 37 °C for 14 days. The samples were compared before and after soaking. The obtained results showed growth of new phases containing calcium in all prepared films.*

**Key words:** *chitosan, montmorillonite, composites, surface properties, microscopy, SBF soaking.*

**Received:** 15.02.2017

**Accepted:** 01.06.2017

## 1. Introduction

In this paper, chitosan samples of different molecular weights and a composite of chitosan with montmorillonite were prepared as a material designed for tissue engineering applications. It is well known that chitosan, a hydrophilic polysaccharide, has unique properties, such as its bioactivity, biodegradability, biocompatibility and non-toxicity to humans, and it is used for various biomedical applications [1–3]. Therefore, chitosan can be considered as a good candidate for the preparation of new materials for tissue engineering applications. The bioactivity of polymer materials has been typically followed *in vitro* by monitoring the formation of an apatite layer on the surface of the film after being immersed in a simulated body fluid (SBF) solution [4–6].

Therefore, the purpose of this study was to compare the structure and morphology of the prepared films before and after immersing the film in a SBF solution at 37°C for 14 days. The properties of chitosan (Ch) samples and the Ch/MMT composite were investigated using scanning electron microscopy (SEM), tapping-mode atomic force microscopy (AFM) and attenuated total reflectance Fourier transform infrared spectroscopy (ATR-FTIR). These techniques are useful methods for the study of structure, homogeneity and intermolecular interactions of polymer materials [7–9].

## 2. Materials and Methods

### 2.1 Materials

Chitosan samples have a degree of deacetylation of 79% with a viscosity average molecular weight of 590,000 for Ch I and of 1,400,000 for Ch II. Both chitosan samples and montmorillonite were supplied by Aldrich, Poland. An aqueous solution of 1.0 wt% was prepared by dissolving chitosan powder in acetic acid solution (1 wt%). A composite of chitosan with montmorillonite was obtained by drop casting a suspension of montmorillonite (3% relative to chitosan) and polymer (1 wt%) in 1 % acetic acid. Polymer films were obtained by the solution casting method.

The *in vitro* bioactivity of films was assessed by their *in vitro* apatite-forming ability on the surface of films during storage in SBF solution [4]. Samples (10 mm x 10 mm) were immersed in 15 mL of SBF and stored at 37°C for periods of up to 14 days. SBF solution was prepared according to Kokubo's SBF solution [4] using the standard ion composition ( $\text{Na}^+$  142.0 mM,  $\text{K}^+$  5.0 mM,  $\text{Mg}^{2+}$  1.5 mM,  $\text{Ca}^{2+}$  2.5 mM,  $\text{Cl}^-$  147.8 mM,  $\text{HCO}_3^-$  4.2 mM,  $\text{HPO}_4^{2-}$  1.0 mM, and  $\text{SO}_4^{2-}$  0.5 mM), buffered at the physiological pH of 7.40 at 37°C, with tris(hydroxymethyl)aminomethane and hydrochloric acid. After 7 and 14 days, samples were removed from the SBF solution, washed with distilled water and stored in a desiccator prior to SEM, AFM and ATR-FTIR analyses.

### 2.2 Methods

Topographic imaging was performed in air using a multimode scanning probe microscope with a Nanoscope IIIa controller (Digital Instruments Santa Barbara, CA) operating in the tapping mode, at room temperature. Surface images, using scan widths ranging from 1  $\mu\text{m}$  to 10  $\mu\text{m}$ , with a scan rate of 1.97 Hz were acquired at a fixed resolution (512 x 512 data points). The roughness parameter measured as the root mean square ( $R_q$ ) was calculated for the scanned area (5  $\mu\text{m}$  x 5  $\mu\text{m}$ ) using Nanoscope software.

Sample morphology was investigated by scanning electron microscopy (SEM) Quanta 3D FEG, D9399, FEI Company, the Netherlands.

FTIR spectra of the used chitosan sample and its composites were recorded on Genesis II FTIR spectrophotometer Mattson (USA) equipped with an ATR device (MIRacleTM

PIKE Technologies) with zinc selenide (ZnSe) crystal, in the wavelength range between 4000 and 400  $\text{cm}^{-1}$ , at a resolution of 2  $\text{cm}^{-1}$  and 60-times scanning. The samples were prepared from 1% solutions. All spectra were obtained for films of similar thickness.

### 3. Results and Discussion

The surface morphology of films obtained for chitosan samples and the composition of chitosan with montmorillonite were observed using atomic force microscopy (AFM) and scanning electron microscopy (SEM). Examples of AFM images for chitosans and Ch/MMT composites are shown in Figures 1 and 2. The corresponding roughness values are presented in Table 1.

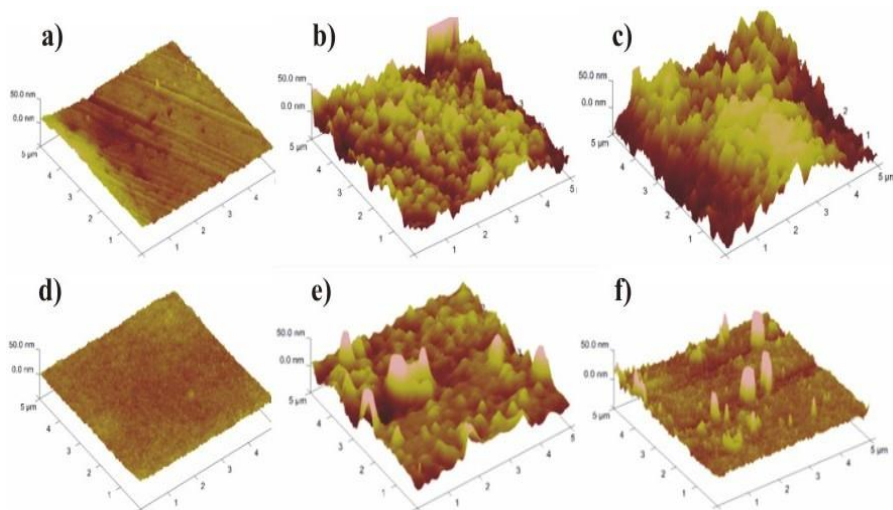


**Figure 1.** AFM images of the surface of films before and after immersion in SBF: a) Ch I before immersion, b) Ch I after 1 week, c) Ch I after 2 weeks, d) Ch II before immersion, e) Ch II after 1 week, f) Ch II after 2 weeks.

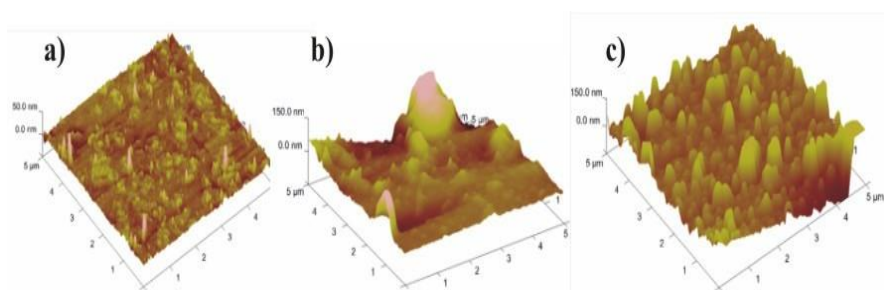


**Figure 2.** AFM images of the surface of films made of Ch/MMT: a) before immersion, b) after 1 week, c) after 2 weeks of immersion.

**Table 1.** The roughness parameters ( $R_q$ ) for films of different compositions

Sample	$R_q$ (nm)
Ch I 0	2.80
Ch I 1 week	13.8
Ch I 2 weeks	24.4
Ch II 0	2.31
Ch II 1 week	11.7
Ch II 2 weeks	8.98
Ch/MMT 0	4.03
Ch/MMT 1 week	37.9
Ch/MMT 2 weeks	45.9

As shown in Figures 1a and 1d, the pure chitosan films had the smoothest surfaces. This agrees with the value of the roughness parameter, which is about 3 nm (Table 1). For the chitosan/MMT composite film, the film surfaces became rougher than before the addition of MMT, and the values of the roughness parameters increased (Table 1). These results are in good agreement with previously reported values for chitosan composites [7–10]. The *in vitro* mineralisation behaviour of chitosans and the chitosan/MMT composite was evaluated by immersing them in a SBF solution for up to 14 days. The tested materials did not dissolve after immersion in the SBF solution and kept their shape. As shown in Figures 1b–c, 1e–f and 2b–c, the surface of all films was altered by growth of new phases. The AFM images illustrate an increasing number and height of peaks on the film surface. The film surfaces became rougher than before immersion in SBF solution and the values of the roughness parameters increased (Table 1). The growth of new phase was the highest for the chitosan composite. The roughness of films increased with increasing immersion period up to 14 days.

Figures 3 and 4 show SEM microphotographs of the top surfaces of the polymer and composite films before and after immersion in SBF solution, respectively. It could be observed that before immersion, the pure chitosans and composite films showed a relatively smooth surface morphology, except for some small undulations in the longitudinal direction (Figures 3a, 3d and 4a). After 7 days of immersion, the films showed calcium phosphate spread (Figures 3b, 3e and 4b) in the early stages of deposition. After immersion for 14 days, the films showed increased calcium phosphate deposits on the surface, demonstrating a process of deposit growth (Figures 3c, 3f and 4c). In the case of Ch II, the increase of the new phase was rather low (Figures 3d–f). The largest increase was observed for the Ch I and composite films. The observed changes in the SEM data are in agreement with the AFM results.

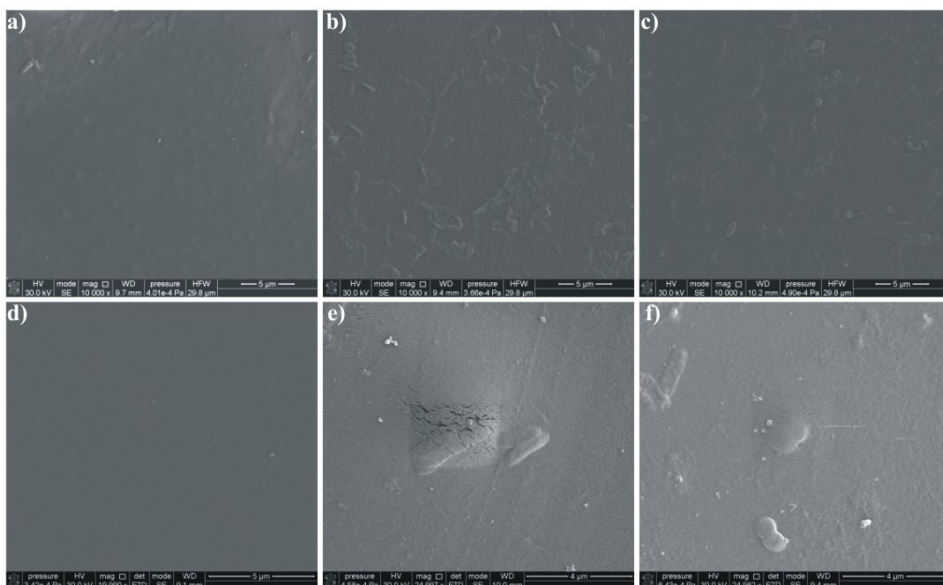


**Figure 3.** Morphology of the surface of films before and after immersion in the SBF. a) Ch I before immersion, b) Ch I after 1 week, c) Ch I after 2 weeks, d) Ch II before immersion, e) Ch II after 1 week, f) Ch II after 2 weeks.

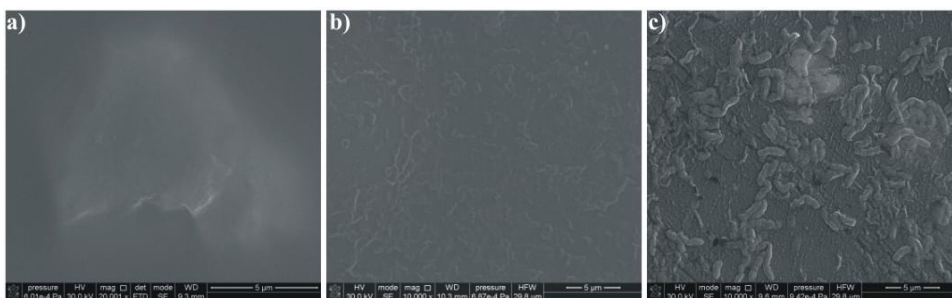


**Figure 4.** Morphology of the surface films made of Ch II/MMT: a) before immersion, b) after 1 week, c) after 2 weeks of immersion.

Evolution of new phase formation was also analysed by ATR-FTIR analysis (Figure 5). Before immersion in a SBF solution, the spectra presented some peaks between  $1000\text{ cm}^{-1}$  and  $1200\text{ cm}^{-1}$ , representatives of the skeletal vibration of saccharide rings, bands at  $1552\text{ cm}^{-1}$  (amide II) and  $1642\text{ cm}^{-1}$  (amide I) and strong absorption bands at the frequency range of  $3200\text{--}3400\text{ cm}^{-1}$ , which is characteristic of chitosan. After 2 weeks of immersion, the spectra exhibited peaks at  $1030\text{ cm}^{-1}$ ,  $1000\text{ cm}^{-1}$  and  $667\text{ cm}^{-1}$ , corresponding to different modes of  $\text{PO}_4^{3-}$  groups in apatite [11, 12]. Broadening of the peak at  $1030\text{ cm}^{-1}$  revealed the presence of a polymer and its interaction with  $\text{PO}_4^{3-}$  groups. The changes in the  $1300\text{--}1460\text{ cm}^{-1}$  range and about  $894\text{ cm}^{-1}$  were due to the carbonate ions in apatite [11]. Thus, the ATR-FTIR spectra of films exhibited characteristic phosphate and carbonate bands, which provide evidence of the formation of an apatite layer.

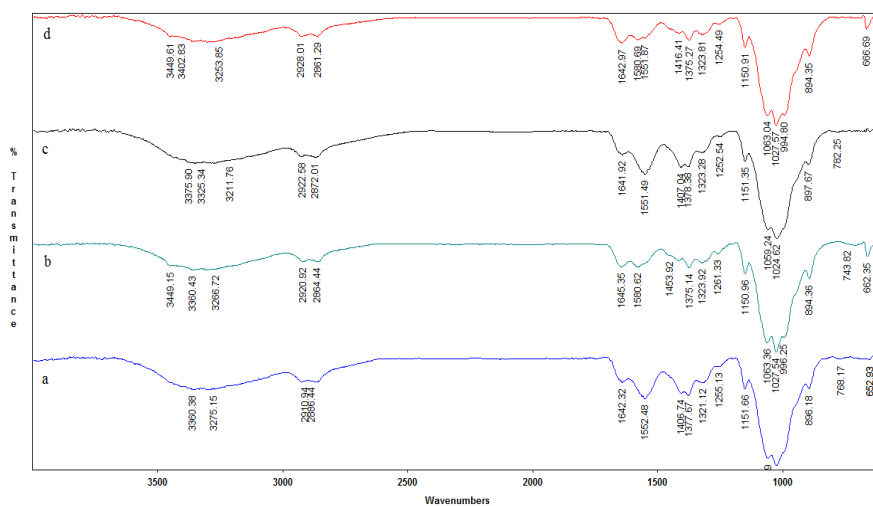


**Figure 5.** ATR-infrared spectra of chitosan and Ch/MMT composite films before and after immersion in SBF: a) chitosan before immersion, b) chitosan after 2 weeks, c) composite before immersion, d) composite after 2 weeks.

#### 4. Conclusions

In the presented study, the structure and morphology of chitosans and chitosan/MMT composite films before and after immersion in a SBF solution was studied. Upon immersion in a SBF solution, the used films were able to promote the deposition of the apatite layers. The largest increase was observed for the chitosan sample with relatively low molecular weight and Ch/MMT composite films. The ATR-infrared spectra confirmed the formation of an apatite layer on films of chitosan and composite. In summary, the present investigation has demonstrated that the films are enriched with components of SBF solution.

#### 5. Acknowledgements

*Financial support from the COST Action MP 1301 NEWGEN is gratefully acknowledged.*

#### 6. References

- [1] Dutta PK, Dutta J, Tripath VS; (2004) Chitin and chitosan: Chemistry, properties and applications. *J Sci Ind Res* 63, 20–31.
- [2] Rinaudo M; (2008) Main properties and current applications of some polysaccharides as biomaterials. *Polym Int* 57, 397–430. DOI: 10.1002/pi.2378
- [3] Katti KS, Katti DR, Dash R; (2008) Synthesis and characterization of a novel chitosan/montmorillonite/hydroxyapatite nanocomposite for bone tissue engineering. *Biomed Mater* 3, 1–12. DOI: 10.1088/1748-6041/3/3/034122
- [4] Kokubo T, Takadama H; (2006) How useful is SBF in predicting in vivo bone bioactivity? *Biomaterials* 27, 2907–2915. DOI: 10.1016/j.biomaterials.2006.01.017

- [5] Baskar D, Balu R, Kumar TS; (2011) Mineralization of pristine chitosan film through biomimetic process. *Int J Biol Macromol* 49, 385–389. DOI: 10.1016/j.ijbiomac.2011.05.021
- [6] Caridade SG, Merino EG, Alves NM, Bermudez VZ, Boccaccini AR, Mano JF; (2013) Chitosan membranes containing micro or nano-size bioactive glass particle: evolution of biomineralization followed by *in situ* dynamic mechanical analysis. *J Mech Behav Biomed Mater* 20, 173–183. DOI: 10.1016/j.jmbbm.2012.11.012
- [7] Xu Y, Ren X, Hanna MA; (2006) Chitosan/clay nanocomposite film preparation and characterization. *J Appl Polym Sci* 99, 1684–1691. DOI: 10.1002/app.22664
- [8] Chivrac F, Pollet E, Avérous L; (2009) Progress in nano-biocomposites based on polysaccharides and nanoclays. *Mater Sci Eng R* 67, 1–17. DOI: 10.1016/j.mser.2009.09.002
- [9] Sahoo D, Naya PL; (2012) Synthesis and characterization of chitosan/cloisite 30B film for controlled release of ofloxacin. *J Appl Polym Sci* 123, 2588–2594. DOI: 10.1002/app.34595
- [10] Lewandowska K; (2015) Characterization of chitosan composites with synthetic polymers and inorganic additives. *Int J Biol Macromol* 81, 159–164. DOI: 10.1016/j.ijbiomac.2015.08.003
- [11] Yousefpour M, Afshar A, Yang X, Li X, Yang B, Wu Y, Chen J, Zhang X; (2006) Nano-crystalline growth of electrochemically deposited apatite coating on pure titanium. *J Electroanal Chem* 589, 96–105. DOI: 10.1016/j.jelechem.2006.01.020
- [12] Yan Y, Zhang X, Li C, Huang Y, Ding Q, Pang X; (2015) Preparation and characterization of chitosan-silver/hydroxyapatite composite coating on TiO<sub>2</sub> nanotube for biomedical applications. *Appl Surf Sci* 332, 62–69. DOI: 10.1016/j.apsusc.2015.01.136